Bioconjugate Chemistry

Article

pubs.acs.org/bc

Synthesis and Characterization of a High-Affinity NOTA-Conjugated Bombesin Antagonist for GRPR-Targeted Tumor Imaging

Zohreh Varasteh,[†] Irina Velikyan,[†,‡,§] Gunnar Lindeberg,[∥] Jens Sörensen,[‡,§] Mats Larhed,[∥] Mattias Sandström,[§] Ram Kumar Selvaraju,[†] Jennie Malmberg,[†] Vladimir Tolmachev,[‡] and Anna Orlova*[,†]

[†]Preclinical PET Platform and [∥]Organic Pharmaceutical Chemistry, Department of Medicinal Chemistry, Faculty of Pharmacy, and [‡]Biomedical Radiation Sciences, Department of Radiology, Oncology and Radiation Science, Faculty of Medicine, Uppsala University, Uppsala, Sweden

[§]PET Centrum, Uppsala University Hospital, Uppsala, Sweden

Supporting Information

ABSTRACT: The gastrin-releasing peptide receptor (GRPR/BB2) is a molecular target for the visualization of prostate cancer. This work focused on the development of high-affinity, hydrophilic, antagonistic, bombesin-based imaging agents for PET and SPECT. The bombesin antagonist analog D-Phe-Gln-Trp-Ala-Val-Gly-His-Sta-Leu-NH_2 ([D-Phe^6,Sta^{13},Leu^{14}]-bombesin[6−14]) was synthesized and conjugated to 1,4,7-triazacyclononane-*N*,*N*′,*N*″-triacetic acid (NOTA) via a diethylene glycol (PEG_2) linker. The resulting conjugate, NOTA-PEG_2-[D-Phe^6,Sta^{13},Leu^{14}]bombesin[6−14] (NOTA-P2-RM26), was labeled with ^{68}Ga ($T_{1/2}$ = 68 min, positron emitter) and ^{111}In ($T_{1/2}$ = 2.8 days, gamma emitter). The labeling stability, specificity, inhibition efficiency (IC_{50}), and dissociation constant (K_D) of both labeled compounds as well as their cellular retention and internalization were investigated. The pharmacokinetics of the dual isotope (^{111}In/^{68}Ga)-labeled peptide in both normal NMRI mice and PC-3 tumor-bearing Balb/c nu/nu mice was also studied. NOTA-P2-RM26 was labeled with ^{111}In and ^{68}Ga at a radiochemical yield of >98%. Both conjugates were shown to have high specificity and binding affinity for GRPR. The K_D value was determined to be 23 ± 13 pM for the ^{111}In-labeled compound in a saturation binding experiment. In addition, ^{nat}In- and ^{nat}Ga-NOTA-P2-RM26 showed low nanomolar binding inhibition concentrations (IC_{50} = 1.24 ± 0.29 nM and 0.91 ± 0.19 nM, respectively) in a competitive binding assay. The internalization rate of the radiolabeled conjugates was slow. The radiometal-labeled tracers demonstrated rapid blood clearance via the kidney and GRPR-specific uptake in the pancreas in normal mice. Tumor targeting and biodistribution studies in mice bearing PC-3 xenografts displayed high and specific uptake in tumors (8.1 ± 0.4%ID/g for ^{68}Ga and 5.7 ± 0.3%ID/g for ^{111}In) and high tumor-to-background ratios (tumor/blood: 12 ± 1 for ^{68}Ga and 10 ± 1 for ^{111}In) after only 1 h p.i. of 45 pmol of peptide. The xenografts were visualized by gamma and microPET cameras shortly after injection. In conclusion, the antagonistic bombesin analog NOTA-PEG_2-D-Phe-Gln-Trp-Ala-Val-Gly-His-Sta-Leu-NH_2 (NOTA-P2-RM26) is a promisindg candidate for prostate cancer imaging using PET and SPECT/CT.

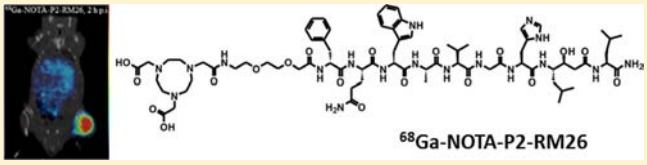

INTRODUCTION

Prostate cancer is, in most cases, a slow-growing cancer, and symptoms arise only when the tumor has already spread out of the local gland. Thus, patients often have metastatic disease at the time of diagnosis.[1] Staging, the detection of bone and soft tissue involvement, is essential for guiding optimal therapy. The selection of treatment options highly depends on the stage of the cancer. Radical prostatectomy and/or external radiation therapy are the treatment modalities used for early diagnosed, locally confined prostate tumors, whereas androgen deprivation therapy (ADT) is the first-line treatment for the palliation of symptomatic, late stage prostate cancer that has already metastasized.[2,3]

PC cells show tropism for bone, which is a strongly preferred site for the spread of this cancer. Bone scans using ^{99m}Tc-methylene diphosphonate are the initial, most sensitive, and most cost- and time-efficient imaging modality for the metastatic evaluation of PC.[4] Clinically, the imaging of soft tissue metastases remains a significant problem for the staging of this disease.

Radionuclide-based molecular imaging allows practitioners to obtain local information from primary tumors as well as to determine the extent of the disease. Overexpression of GRPR was found in 63−100% of prostate primary tumors and over 50% of lymph and bone metastases.[5] High receptor density was observed in androgen-dependent,[6] lower-grade, and smaller-sized tumors.[7] The expression pattern of GRPR in PC suggests that this receptor might serve as an imaging target for the detection of PC extracapsular extensions and local soft tissue metastases.[8]

Received: December 10, 2012
Revised: June 3, 2013
Published: June 12, 2013

dx.doi.org/10.1021/bc300659k | *Bioconjugate Chem.* 2013, 24, 1144−1153

Chart 1. Structural Formula of NOTA-PEG$_2$-[D-Phe^6,Sta^{13},Leu^{14}]bombesin[6-14] (NOTA-P2-RM26)

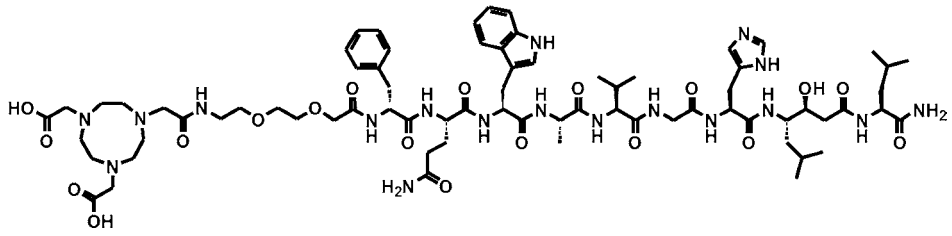

GRPR (also referred to as BB2) is a member of the bombesin receptor family in mammals, together with the neuromedin B receptor (NMBR/BB1) and the bombesin receptor subtype 3 (BB3) and subtype 4 (BB4, only in amphibians). Bombesin receptors are G protein-coupled receptors that are activated by BN and/or bombesin-like peptides.[9] BN, which has two mammalian homologues, neuromedin B (NMB)[10] and GRP,[11] is a linear tetradecapeptide and has high affinity for GRPR. BN-based tracer agonists have been extensively investigated in preclinical[12,13] and clinical studies.[14,15] All of these agonists demonstrate a high binding affinity for GRPR and good radioligand internalization properties, which are essential factors for optimal imaging. However, agonist-based bombesin analogs demonstrate strong physiological potency and mitogenicity even in trace amounts[16] as well as high and maintained uptake in normal GRPR-positive organs and liver (if lipophilic linker was used),[17] which results in images with poor contrast. It was suggested that antagonistic BN analogs with tumor growth inhibitory effects, which have been introduced recently,[18,19] could overcome these drawbacks (reviewed in refs 20,21). Despite a very low internalization rate, somatostatin receptor antagonists have higher and more well-retained tumor uptake than the equipotent agonists.[22] This phenomenon has also been detected for bombesin analogs. BN-based antagonists were shown to have superior *in vivo* biodistribution and targeting properties compared to agonists.[23] In addition, it was reported that GRPR antagonists have more binding sites than agonists, which may make them preferable to agonists for *in vivo* tumor targeting.[24] More binding sites for radioconjugates may enhance localization accuracy, especially in small lesions and tumors with low receptor expression. Both high affinity and a low dissociation rate are important contributors to the superiority of analogs with antagonistic functions.

The aim of the present study was to develop a high-affinity imaging agent for PC staging that had optimal pharmacokinetics and was based on a nine-amino-acid bombesin analog, D-Phe-Gln-Trp-Ala-Val-Gly-His-Sta-Leu-NH$_2$ (RM26).[20] RM26 variants modified with DOTA as a chelator and glycine-4-aminobenzoyl[24] or 4-amino-1-carboxymethyl-piperidine[25] as a spacer have been previously investigated. In this study, NOTA, which forms a stable complex with ^{68}Ga,[26] was coupled to the peptide via a synthetic polymer, diethylene glycol (PEG$_2$), to decrease the lipophilicity of the conjugate and to modulate its pharmacokinetics. In addition, the peptide was labeled with radiometals suitable for PET and SPECT (^{68}Ga and ^{111}In, respectively).

MATERIAL AND METHODS

Peptide Synthesis. The bombesin analog NOTA-PEG$_2$[D-Phe^6,Sta^{13},Leu^{14}]bombesin[6−14] (further denoted as NOTA-P2-RM26, see Chart 1) was synthesized by standard manual solid-phase peptide synthesis,[27] as described in Supporting Information.

Radiolabeling and in Vitro Stability Test. A ^{68}Ge/^{68}Ga generator (50 mCi, Obninsk, Eckert and Ziegler) was eluted with 1 mL fractions of 0.1 M HCl (Merck). The second fraction (200 MBq) was buffered with sodium acetate (0.2 M, pH 4.6, 200 μL) and sodium hydroxide (10 M, 10 μL) to ensure a pH of 4.2−4.6, followed by the addition of an aqueous solution of NOTA-P2-RM26 (10 nmol, 10 μL in Milli-Q water). The mixture was incubated at 75 °C for 10 min. The crude product was analyzed by HPLC (Beckman), with UV and radioactivity detectors coupled in series and using a column packed with SOURCE 15RPC chromatography polymeric medium (Resource RPC, 17−1181−01, GE Healthcare). The acquired data were analyzed with the Beckman System Gold Nouveau chromatography software package. The reaction mixture was also analyzed by radio-ITLC (Biodex Medical Systems) with running buffer containing 0.2 M citric acid (pH 2.0) (R_f = 0.0 for the peptide and R_f = 1.0 for the free radiometal) and pyridine:acetic acid:water (5:3:1.5) (R_f = 0.9 for the peptide and R_f = 0.0 for the free radiometal). The distribution of radioactivity on the strips was measured with a Cyclone storage phosphor imaging system and analyzed using OptiQuant image analysis software (Perkin-Elmer Sweden AB).

For ^{111}In labeling, an aqueous solution of NOTA-P2-RM26 (10 nmol, 10 μL in Milli-Q water) and 80 μL of 0.2 M ammonium acetate (pH 5.5) (Merck) were mixed with 60 MBq (80−150 μL in 0.05 M hydrochloric acid) of ^{111}In (Covidien) and incubated at 75 °C for 30 min. The buffers for ^{111}In labeling were purified from metal contamination using Chelex 100 resin (Bio-Rad Laboratories). Radio-ITLC analysis was performed on a small aliquot of the reaction mixture as described above.

For metal loading, an aqueous solution of 14 nmol of ^{nat}GaCl$_3$ (14 μL) or 13.5 nmol of ^{nat}InCl$_3$ (13.5 μL) (Sigma-Aldrich) was added to 10 nmol of NOTA-P2-RM26 (10 μL) using the same protocol described for the radioactive isotopes.

To evaluate the labeling stability, ^{68}Ga-NOTA-P2-RM26 and ^{111}In-NOTA-P2-RM26 were challenged with a 500-fold molar excess of EDTA disodium salt (Sigma) and incubated for 1 h at RT. The samples were analyzed by radio-ITLC. Additionally, the samples were analyzed by SDS-PAGE, and free radiometals were applied as low molecular weight internal references in another well on the same gel.

To test the stability of the peptide in serum, 5 nmol of radiolabeled NOTA-P2-RM26 was incubated in 0.5 mL murine serum at 37 °C for 1 h. The samples were analyzed by ITLC and SDS-PAGE.

In Vitro Studies. The GRPR-expressing human prostate cancer cell line PC-3 (ATCC, LGC Standards AB) was cultured in RPMI medium supplemented with 10% FCS, 2 mM L-glutamine and PEST (100 IU/mL penicillin) (all from Biochrom AG).

dx.doi.org/10.1021/bc300659k | Bioconjugate Chem. 2013, 24, 1144−1153

This medium is referred to as complete medium in the text. All experiments were performed in triplicate. One million cells per dish were seeded one day before the experiment.

In Vitro Binding Specificity Assay. The binding specificity of radiolabeled NOTA-P2-RM26 to PC-3 cells was tested by incubating the cells with 1 nM of the ^{68}Ga- or ^{111}In-NOTA-P2-RM26 solution for 2 h at 4 °C. To one set of dishes, a 100-fold excess of unlabeled NOTA-P2-RM26 was added 5 min before the addition of ^{68}Ga- or ^{111}In-NOTA-P2-RM26. After incubation, the cells were detached using 0.5 mL of a 25% trypsin/0.02% EDTA solution in buffer (Biochrom AG) and collected. The cell-associated radioactivity was measured in an automated gamma-counter with a 3-in. NaI(Tl) detector (1480 WIZARD, Wallac Oy).

Cellular Processing Assay. To study cellular processing, PC-3 cells were incubated at 37 °C (5% CO_2) with 1 nM ^{111}In-NOTA-P2-RM26 in complete medium. At predetermined time points, the membrane-bound and internalized radioactivity was estimated as previously described.[28]

Internalization Assay. The internalization of ^{68}Ga-NOTA-P2-RM26 and ^{111}In-NOTA-P2-RM26 was compared with that of ^{125}I-Tyr^4-BBN (PerkinElmer) by analyzing the internalized radioactivity after the PC-3 cells were incubated with a 2 nM solution of the labeled conjugates for 30 min at 37 °C.

In Vitro Competitive Binding Assay; IC_{50} Determination. An *in vitro* competitive binding assay was performed using ^{125}I-Tyr^4-BBN. The half maximal inhibitory concentration (IC_{50}) was determined for nonlabeled, ^{nat}Ga-loaded and ^{nat}In-loaded conjugates. Cell monolayers were incubated for 5 h at 4 °C with 0.1 pmol of ^{125}I-Tyr^4-BBN in the presence of increasing concentrations of competitor ($(0-1) \times 10^{-6}$ M). After incubation, the cells were collected, and their radioactivity was measured.

Real-Time Ligand Binding and Receptor Saturation Assay; K_D Determination. The binding of ^{111}In-NOTA-P2-RM26 was measured in real-time at RT using LigandTracer Yellow (Ridgeview Instruments AB), as described previously.[29,30] Two radioligand concentrations were used (0.5 and 10 nM). Uptake was monitored for 200 min, and retention was monitored for 1300 min. Interaction analysis and calculation of the equilibrium dissociation constant (K_D) were performed with TracerDrawer software (Ridgeview Instruments AB).

Binding Site Quantification; B_{Max} Determination. PC-3 cells were incubated with 20 nM of ^{68}Ga- or ^{111}In-NOTA-P2-RM26 at RT (LigandTracer Yellow) or 27 nM of ^{125}I-Tyr^4-BBN at 4 °C (LigandTracer Gray). When the radioactivity uptake reached saturation, the cells were washed twice with serum-free media, and after being trypsinized, the detached cells were counted and collected for radioactivity measurements. The data were used to calculate the number of available binding sites, B_{max}, for each of the compounds on the PC-3 cells.

In Vivo Studies. All animal experiments were planned and performed according to the national legislation on the protection of laboratory animals, and the study plans were approved by the local committee for animal research ethics. Groups of 4 mice per data point were used in all experiments. The biodistribution of ^{68}Ga- and ^{111}In-labeled NOTA-P2-RM26 was evaluated in male NMRI mice (weight: 33.1 ± 1.4 g). BALB/c nu/nu male mice bearing PC-3 xenografts (5×10^6 cells/mouse, implanted 3 weeks before the experiment) were used for the *in vivo* targeting study (weight: 21.4 ± 1.0 g). The average tumor size was 0.3 ± 0.1 g at the time of the experiment.

Biodistribution and in Vivo Binding Specificity in NMRI Mice. Male NMRI mice were coinjected with 23 pmol of ^{68}Ga/^{111}In-NOTA-P2-RM26 (350 kBq of ^{68}Ga and 10 kBq of ^{111}In, 100 μL in PBS) into the tail vein. To test the *in vivo* binding specificity, one group of animals was intravenously preinjected with 20 nmol of unlabeled peptide 1 h before injection with the labeled conjugate. The mice were euthanized at 1, 2, and 24 h p.i. by intraperitoneal injection of a Ketalar-Rompun solution (10 mg/mL Ketalar and 1 mg/mL Rompun; 20 μL of solution per gram of body weight). Blood samples were collected by heart puncture. The organs of interest were collected and weighed, and their radioactivity content was measured using a gamma-counter. Whole gamma spectra were collected for each sample. One day after the first radioactivity measurement (^{68}Ga radioactivity was decayed), the samples were remeasured for ^{111}In radioactivity using the same protocol. Radioactivity in first measurement after subtraction of the ^{111}In decay-corrected radioactivity was considered to be the ^{68}Ga radioactivity. The organ uptake values are expressed as %ID/g.

Effect of the Peptide Dose on the Tumor Uptake and Pharmacokinetics of ^{111}In-NOTA-P2-RM26 in Tumor-Bearing Mice. To study the influence of the peptide dose on its tumor uptake and pharmacokinetics, male Balb/c nu/nu mice bearing PC-3 xenografts were injected with ^{111}In-NOTA-P2-RM26 (30 kBq, 100 μL in PBS). The administered peptide dose was adjusted to 3.6, 15, 25, or 45 pmol/mouse by diluting with nonlabeled NOTA-P2-RM26. The mice were sacrificed 2 h p.i. The radioactivity content of the blood and selected organs was measured using the ^{111}In protocol and expressed as described earlier.

Biodistribution and in Vivo Binding Specificity in Balb/c nu/nu Mice Bearing PC-3 Prostate Cancer Xenografts. To study tumor targeting, male BALB/c nu/nu mice bearing PC-3 xenografts were intravenously injected with 45 pmol of ^{68}Ga/^{111}In-NOTA-P2-RM26 (350 kBq of ^{68}Ga and 10 kBq of ^{111}In, 100 μL in PBS). The mice were euthanized at 1, 3, or 24 h p.i., and the organ radioactivity content was measured and evaluated as described above. To test the *in vivo* binding specificity, a group of animals was coinjected with 20 nmol of unlabeled peptide. For the animals in this blocked group, only the blood, pancreas, and tumors were collected at 1 h p.i.

Imaging Studies. Tumor-bearing mice were injected with 45 pmol of ^{111}In-NOTA-P2-RM26 (260 kBq) or ^{68}Ga-NOTA-P2-RM26 (300 kBq). The ^{111}In-NOTA-P2-RM26-injected animals were sacrificed 3 h p.i. and scanned with a clinical gamma camera (Siemens e.cam) equipped with a MEGP collimator. For ^{68}Ga-NOTA-P2-RM26, images were acquired at 1 and 2 h p.i. using a micro-PET/CT (Gamma Medica Inc.). The PET and CT data were fused and analyzed using PMOD v3.13 (PMOD Technologies Ltd.).

Data Analysis and Statistics. The data were analyzed with unpaired two-tailed *t*-tests using GraphPad Prism (version 4.0 for Windows GraphPad Software) to differentiate significant differences ($p < 0.05$). For the dual labeling experiments, paired tests were used.

RESULTS

Peptide Synthesis. NOTA-P2-RM26 was synthesized and purified as described in the Supporting Information 1. Lyophilization of the appropriate fractions from the HPLC purification afforded 9.2 mg of purified product, corresponding to a total yield of 44% (based on the initial loading of the resin). HPLC/MS analysis of the final product using a Kinetex 2.6 μm C18 (50 × 3.0 mm) column and a 2.5 min, 5−60% acetonitrile/water (0.05% formic acid) gradient gave an *m/z*

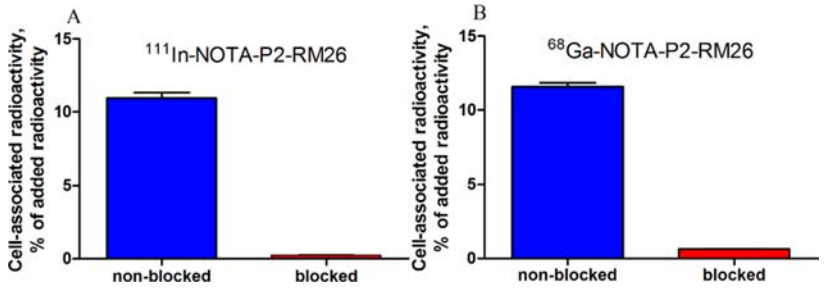

Figure 1. *In vitro* specificity test of ^{111}In- and ^{68}Ga-NOTA-P2-RM26 for PC-3 cells. The radiolabeled conjugates were added to cultured PC-3 cells at a concentration of 1 nM. One set of culture dishes in each experiment was pretreated with a 100-fold molar excess of nonlabeled NOTA-P2-RM26 before incubation with the labeled conjugate. Data are presented as the means ± SD of three culture dishes.

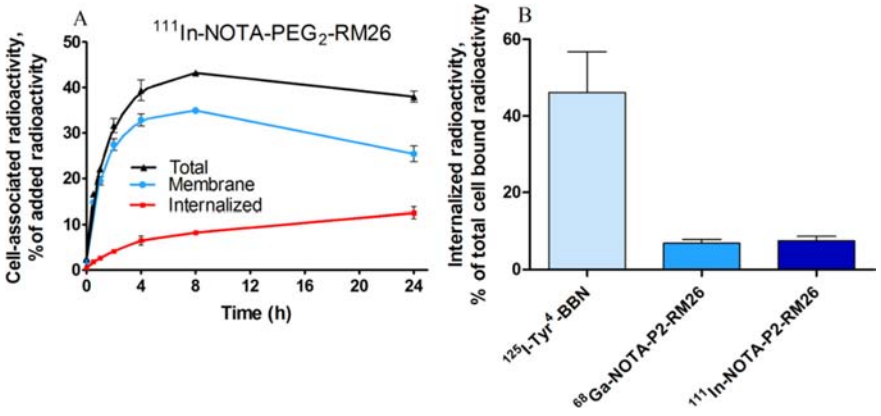

Figure 2. (A) Cellular processing of ^{111}In-NOTA-P2-RM26 by PC-3 cells during continuous incubation with 1 nM of ^{111}In-NOTA-P2-RM26. (B) Internalization of ^{125}I-Tyr^4-BBN (agonist), ^{68}Ga-NOTA-P2-RM26 (antagonist), and ^{111}In-NOTA-P2-RM26 (antagonist) by PC-3 cells. Data are presented as the means ± SD of three culture dishes.

value in accordance with that expected (1544.88). The purity, as determined from the 280 nm trace, was 96.7% (Figure S1).

Radiolabeling and in Vitro Stability Testing. Because of the almost quantitative radiolabeling yield for both ^{111}In-NOTA-P2-RM26 and ^{68}Ga-NOTA-P2-RM26 (98.6 ± 0.6%), these tracers could be used without further purification (Figure S2). A maximum specific radioactivity of 6 GBq/μmol and 20 GBq/μmol was obtained for ^{111}In-NOTA-P2-RM26 and ^{68}Ga-NOTA-P2-RM26, respectively.

After 1 h of incubation at RT with a 500-fold molar excess of EDTA, 95% of the radioactivity for ^{111}In-NOTA-P2-RM26 and more than 97% of the radioactivity for ^{68}Ga-NOTA-P2-RM26 were still associated with the peptide. Furthermore, SDS-PAGE demonstrated high stability for ^{68}Ga-NOTA-P2-RM26 and ^{111}In-NOTA-P2-RM26 after incubation with a 500-fold excess of EDTA or murine serum (Figure S3). SDS-PAGE analysis of the serum samples showed a single radioactivity peak with a path length that equaled the path length of NOTA-P2-RM26. No other peaks were detected, indicating that there was no release of free radiometal, there was no peptidase cleavage of the radiopeptide, and there was no transchelation to serum proteins.

In Vitro Studies. *In Vitro Binding Specificity Assay.* *In vitro* binding specificity tests demonstrated that the binding of ^{111}In- and ^{68}Ga-NOTA-P2-RM26 to PC-3 cells is receptor mediated. Presaturation of the cells with nonlabeled NOTA-P2-RM26 significantly decreased the cell binding of the radiolabeled compounds (Figure 1).

Cellular Processing Assay. The binding of ^{111}In-NOTA-P2-RM26 to the PC-3 cells was rapid, and the cell-associated radioactivity reached a plateau in 4 h, at which time approximately 40% of the added radioactivity was cell associated (Figure 2A). The internalization of the ^{111}In-labeled conjugate was low. After 24 h of incubation, the contribution of the internalized radioactivity to the overall cell-bound radioactivity was only 33 ± 3%.

Internalization Assay. To further assess the internalization properties of the tracers, the internalization rates of ^{68}Ga-NOTA-P2-RM26, ^{111}In-NOTA-P2-RM26, and the agonist ^{125}I-Tyr^4-BBN by the PC-3 cells were compared. After 30 min of incubation at 37 °C, almost 50% of the total cell-bound ^{125}I radioactivity was internalized by the cells, while less than 8% of the ^{68}Ga or ^{111}In radioactivity was internalized (Figure 2B).

In Vitro Competitive Binding Assay; IC_{50} Determination. The IC_{50} values of ^{nat}In-NOTA-P2-RM26 and ^{nat}Ga-NOTA-P2-RM26 were determined to be 1.2 ± 0.3 nM and 0.9 ± 0.2 nM, respectively. These values were more than 4-fold lower than that of nonlabeled-NOTA-P2-RM26 (5 ± 1 nM), indicating an improvement in the affinity of the conjugate upon loading with metal cations (Figure 3).

Real-Time Ligand Binding and Receptor Saturation Assay; K_D Determination. According to the LigandTracer data, the calculated K_D for ^{111}In-NOTA-P2-RM26 was 23 ± 13 pM (Figure S4).

Binding Site Quantification; B_{Max} Determination. The number of binding sites for the antagonists ^{111}In- and ^{68}Ga-NOTA-P2-RM26 was 280 000 ± 14 000 receptors/cell, while the number was significantly lower for the agonist ^{125}I-Tyr^4-BBN (120 000 ± 5000 receptors/cell, $p < 0.05$).

In Vivo Studies. *Biodistribution and in Vivo Binding Specificity in NMRI Mice.* A biodistribution study was performed in NMRI mice to determine the cross-reactivity of the

dx.doi.org/10.1021/bc300659k | Bioconjugate Chem. 2013, 24, 1144−1153

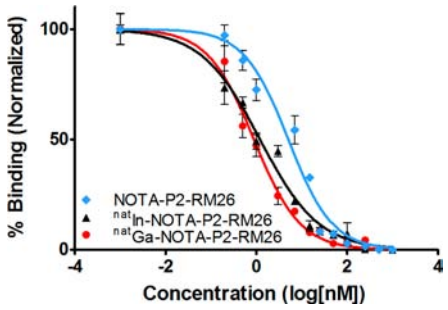

Figure 3. Inhibition of ^{125}I-Tyr^4-BBN binding to PC-3 cells with ^{nat}Ga-NOTA-P2-RM26, ^{nat}In-NOTA-P2-RM26, and nonlabeled NOTA-P2-RM26. Data are the means ± SD of 3 culture dishes.

radioconjugates with murine GRPR in normal organs and to assess their blood and whole body clearance (Figure 4, Table S1). Both radiopeptides showed rapid blood clearance. The liver uptake of both conjugates was low, and a low level of radioactivity was detected in the gastrointestinal tract. The radioactivity uptake in the kidney was also low. Preinjection of 20 nmol of nonlabeled conjugate caused a significant reduction in the radioactivity uptake in the GRPR-positive organs (pancreas, stomach, and small intestine) ($p < 0.05$). In addition, a small but significant reduction in uptake was observed in the blood and spleen for the ^{68}Ga-labeled conjugate and in the liver, spleen, muscle, and bone for the ^{111}In-labeled conjugate. The radioactivity washout from the receptor-positive organs was also rapid: the radioactivity concentration in the pancreas decreased more than 4-fold between 1 and 2 h p.i.

Effect of the Peptide Dose on the Tumor Uptake and Pharmacokinetics of ^{111}In-NOTA-P2-RM26 in Tumor-Bearing Mice. The data on the effect of the injected peptide dose on the biodistribution and tumor-to-organ ratios of ^{111}In-NOTA-P2-RM26 are presented in Figure 5 and Table S2. The results of the biodistribution studies in the NMRI mice and tumor-bearing mice were in good agreement, as both showed high tracer uptake in normal receptor-positive organs. No significant differences in the tumor-to-organ ratios were observed for most of the organs and tissues for peptide doses between 3.6 and 45 pmol (Figure 5B).

Biodistribution and in Vivo Binding Specificity in Balb/c nu/nu Mice Bearing PC-3 Prostate Cancer Xenografts. The biodistribution and tumor targeting of ^{68}Ga/^{111}In-NOTA-P2-RM26 in PC-3-xenografted mice were studied in a dual isotope study, and the results are presented in Figure 6 and Table S3. Both radioconjugates were rapidly cleared from the blood. Low kidney retention and low liver uptake were displayed for the tracers in the tumor-bearing mice. In good agreement with their biodistribution in the NMRI mice, high uptake was observed for the receptor-positive organs. The washout rate from the target-expressing normal tissues was higher than that from the tumors, leading to increasing tumor-to-organ ratios over time. High uptake and long retention of the radioconjugates were observed in the tumors. The uptake in the pancreas (a GRPR-expressing tissue in rodents) and tumors was specific, as shown in the *in vivo* saturation experiment. The pancreas uptake decreased more than 34-fold for the ^{111}In-labeled conjugate and 21-fold for the ^{68}Ga-labeled conjugate in animals that were coinjected with an excess of nonlabeled peptide. The tumor radioactivity was reduced from 6.0 ± 0.3%ID/g to 0.5 ± 0.3% ID/g for ^{111}In-NOTA-P2-RM26 and from 8.1 ± 0.4%ID/g to 0.37 ± 0.05%ID/g for ^{68}Ga-NOTA-P2-RM26 after *in vivo* receptor saturation, which indicates specific GRPR-mediated uptake.

Imaging Studies. The coronal gamma camera scan that was performed 3 h p.i. of ^{111}In-NOTA-P2-RM26 is presented in Figure 7A. The tumor was clearly visualized. The receptor-positive organs in the abdomen and the kidneys could also be seen in the gamma camera image. MicroPET/CT images (Figure 7B and C) were obtained at 1 and 2 h p.i. of ^{68}Ga-NOTA-P2-RM26. Due to the predominant renal excretion of the radioconjugate, high kidney uptake and urinary bladder accumulation were observed at 1 h p.i. In addition, pancreatic uptake was visualized. Rapid washout of the tracers from normal organs, including the kidneys, resulted in a microPET/CT image showing absolutely dominant radioactivity accumulation in the tumor tissue at 2 h p.i.

DISCUSSION

Accurate staging is crucial for the selection of PC treatment. The sensitivity of the existing screening modalities is not sufficient to confirm the presence or extent of disseminated cancer.[31−33] This is especially important for the visualization of soft tissue metastases. In many cases, this lack of sensitivity leads to the understaging and overtreatment of PC patients.[34] The overexpression of GRPR in human PC suggests that this receptor can be used for visualization and as a therapeutic molecular target in PC patients, especially in the targeting of soft tissue metastases.[9] The progression of PC leads to the transition of androgen-responsive tumor growth toward hormone-refractory

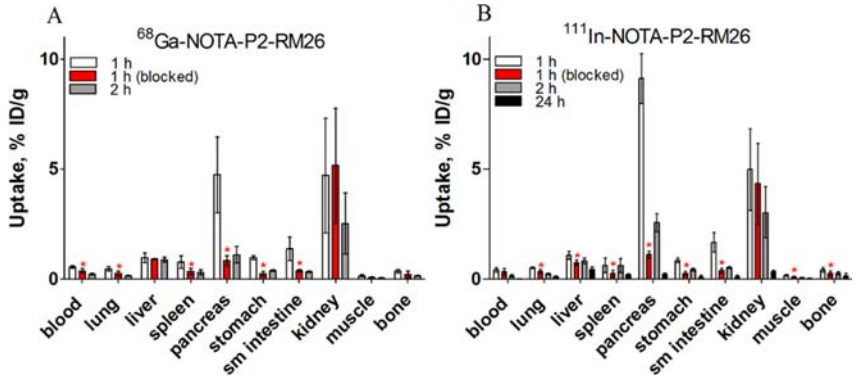

Figure 4. (A) Biodistribution of ^{68}Ga-NOTA-P2-RM26 and (B) ^{111}In-NOTA-P2-RM26 in male NMRI mice at different time points in a dual isotope study (total injected mass of 23 pmol). Data are presented as the mean percentage of the injected dose per gram of tissue (%ID/g ± SD, $n = 4$). The red asterisks denote significant differences between the blocked and nonblocked animals ($p < 0.05$).

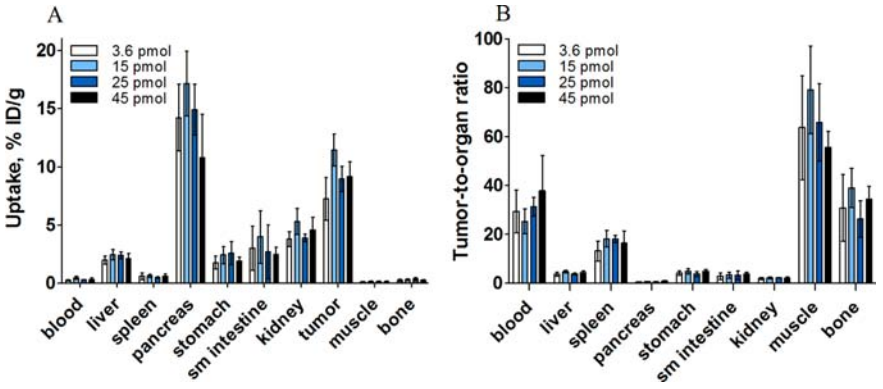

Figure 5. Dose escalation study of ^{111}In-NOTA-P2-RM26 in male BALB/c nu/nu mice bearing PC-3 xenografts. (A) Biodistribution and (B) tumor-to-organ ratio at 2 h after the injection. Data are presented as the mean percentage of the injected dose per gram of tissue (%ID/g ± SD, n = 4).

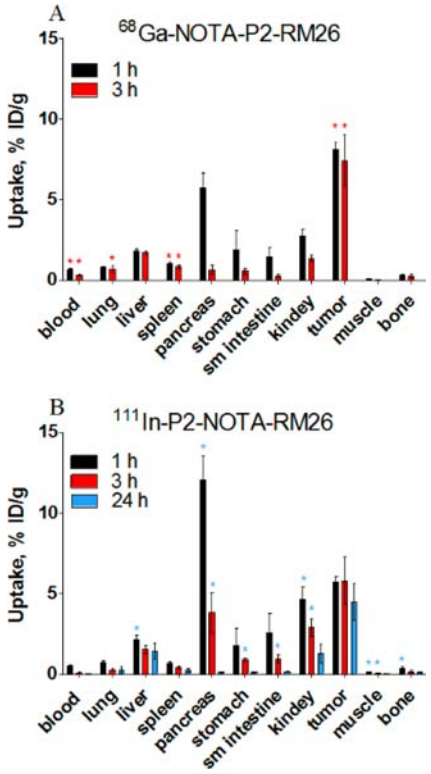

Figure 6. Biodistribution of ^{68}Ga-NOTA-P2-RM26 (A) and ^{111}In-NOTA-P2-RM26 (B) in male BALB/c nu/nu mice bearing PC-3 xenografts at different time points in a dual isotope study (total injected mass of 45 pmol). Data are presented as the mean percentage of the injected dose per gram of tissue (%ID/g ± SD, n = 4). The red asterisks indicate that the ^{68}Ga-NOTA-P2-RM26 uptake was significantly higher than that of ^{111}In-NOTA-P2-RM26 at the same time point (p < 0.05). The blue asterisks indicate that the ^{111}In-NOTA-P2-RM26 uptake was significantly higher than that of ^{68}Ga-NOTA-P2-RM26 at the same time point (p < 0.05).

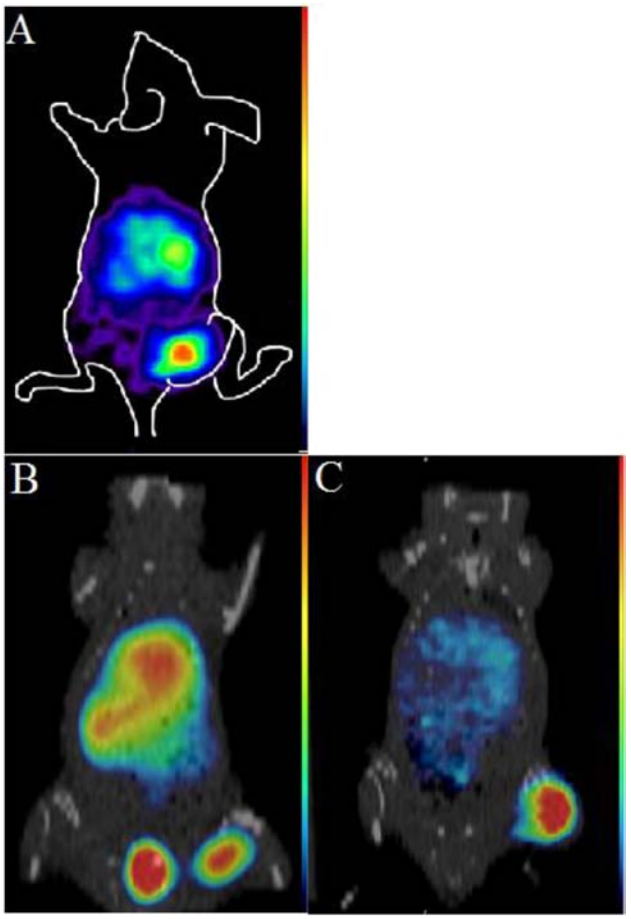

Figure 7. Imaging of GRPR expression in PC-3 xenografts in BALB/c nu/nu male mice. The animal used for the gamma camera imaging (A) was injected with 45 pmol of ^{111}In-NOTA-P2-RM26 (260 kBq) and euthanized at 3 h p.i. The micro-PET/CT images were acquired at 1 h (B) and 2 h (C) p.i. of 45 pmol of ^{68}Ga-NOTA-P2-RM26 (300 kBq).

prostate cancer (HRPC). It has been reported that prostate tumors present different expression levels of GRPR at different stages in tumor progression. Overexpression of GRPR is found in early stage and androgen-dependent prostate tumors, whereas low receptor-mediated binding of radiolabeled-bombesin analogs is observed for androgen-independent PC xenografts.[35] These results suggest that GRPR may be a favorable target for the imaging and treatment of early stage PC tumors.

In this study, we synthesized the NOTA-conjugated bombesin antagonist D-Phe-Gln-Trp-Ala-Val-Gly-His-Sta-Leu-NH_2. PEG_2 was used as a linker to conjugate the chelator NOTA to the peptide. Adding to the overall hydrophilicity, PEG provided favorable pharmacokinetic properties to the peptide, as manifested in the low liver radioactivity uptake and rapid radioactivity excretion in normal GRPR-positive organs. NOTA will be suitable for labeling with many PET radionuclides, such as ^{68}Ga,[26,36] and ^{64}Cu,[37] as well as ^{18}F using AlF,[36,38] in future studies.

The peptide was stably radiolabeled with ^{111}In and ^{68}Ga, with high labeling yields and specific radioactivities, which permitted

dx.doi.org/10.1021/bc300659k | Bioconjugate Chem. 2013, 24, 1144−1153

the use of the radiolabeled conjugates in *in vitro* and *in vivo* experiments without further purification.

A slow PC-3 cell internalization rate was observed for ^{111}In-NOTA-P2-RM26 up to 24 h. The internalization of ^{68}Ga-NOTA-P2-RM26 and ^{111}In-NOTA-P2-RM26 was 6-fold lower in comparison with the internalization of the agonistic analog ^{125}I-Tyr^4-BBN (Figure 2B), indicating that the antagonistic function of RM26 was preserved after modification.[24]

The binding properties of this new peptide, both nonlabeled and loaded with metal, were studied in a competitive binding assay using ^{125}I-Tyr^4-BBN as a displacement radioligand. The IC_{50} values for the analogs loaded with metals were somewhat lower than for their nonlabeled counterpart. It was previously demonstrated that bombesin agonists with positive charges at their N-termini exhibit higher affinities for GRPR, while negative charges decrease its affinity.[18,39] The overall charge of the complex of dianionic NOTA with indium or gallium is +1.[40] This positive charge explains the greater than 4-fold lower IC_{50} values for the metal-loaded analogs compared with the non-loaded peptide in our study.

^{111}In-NOTA-P2-RM26 showed an affinity (K_D) in the low picomolar range (23 ± 13 pM), and 2-fold more binding sites on the human PC-derived PC-3 cells were recognized by the antagonist peptide in comparison with the ^{125}I-labeled universal agonistic analog. These data were in good agreement with the findings of other researchers.[22,24]

The biodistribution of the ^{111}In- and ^{68}Ga-labeled peptides in normal mice demonstrated the specific uptake of the compounds in the receptor-positive organs in the abdominal area (e.g., the pancreas, stomach, and small intestine). The blocking effect of the nonlabeled peptide in the receptor-expressing organs suggests that this peptide analog has cross-reactivity to murine GRPR. A small reduction in the uptake in other organs (blood, spleen, muscle, and bone) might be due to a reduction in the number of bloodborne radioconjugates dissociating from the GRPR-expressing organs. The kidney was found to be the predominant excretion organ, as the radioactivity uptake in both the liver and the gastrointestinal tract (with content) was low. However, the radioactivity uptake in the kidney was as low as 5 ± 2%ID/g at 1 h p.i., indicating a low degree of reabsorption and rapid excretion.

The influence of the administered peptide dose on its biodistribution and tumor targeting in PC-3-xenografted mice was studied. No significant differences in the tumor-to-organ ratios were found for doses between 3.6 and 45 pmol per mouse, which is in agreement with data published for similar antagonists.[24] In contrast, dose-dependent uptake in GRPR-positive organs was previously found for the bombesin agonists ^{67}Ga-BZH3[41] and AMBA,[42] which resulted in better tumor-to-pancreas ratios when a low specific activity was used. The lack of dependence of the tumor-to-organ ratio on the amount of injected protein together with the antagonistic properties of NOTA-P2-RM26 suggests a wide window for peptide dose administration.

Overall, the biodistribution of ^{111}In-NOTA-P2-RM26 was similar to that of the ^{68}Ga-labeled peptide. Both tracers showed rapid blood and whole body clearance along with specific uptake in tumors and receptor-expressing organs. However, there were some slight differences in the biodistribution of the ^{111}In and ^{68}Ga-labeled peptides, although both exhibited similar IC_{50} values *in vitro*. The ^{111}In-labeled conjugate showed a somewhat more rapid blood clearance, but the significantly higher tumor uptake of the ^{68}Ga-labeled analog resulted in higher tumor-to-organ ratios in comparison with the ^{111}In-labeled tracer. Different blood clearance rates for peptides and proteins labeled with different radiometals using the same chelator are a known phenomenon (for BN analogs, see refs 43,44). We speculate that different coordination geometries could play a role in the degree of binding to blood proteins, thus modulating the exertion rate.

The rapid washout of the tracers from the GRPR-positive organs together with the high retention of the radiolabeled peptide in the tumor xenografts suggest that the antagonist NOTA-P2-RM26 has high potential for the visualization of GRPR-positive tumors, even at very early time points, permitting the use of the short-lived, generator-produced radioisotope ^{68}Ga. The data obtained in this study corroborate data for other bombesin antagonists. Particularly, when bombesin antagonists are compared directly with agonists,[23,24] the tumor uptake of the radioactivity for both agonists and antagonists is relatively stable within 4 h p.i., but the concentration of the radioactivity in the pancreas only decreases for antagonists. More interestingly, it was found that the radioactivity uptake of agonists in the pancreas is stable over time, with a minor release of 10−20% from 1 to 4 h p.i.,[41,45,46] whereas the radioactivity uptake in tumors decreases 2-fold.[41,45] This pharmacokinetic behavior (stable tumor uptake and rapid radioactivity release from GRPR-positive organs) may be due to affinity for murine GRPR and/or differences in the target expression density between tumors and receptor-positive organs. Despite high interspecies homology (>90%) between the murine and human GRPRs,[47] different binding affinities of bombesin analogs have been demonstrated for bombesin receptors in different species.[48] Even small differences in affinity can affect the retention of radioactivity in receptor-positive tissues with respect to mouse GRPR expression and xenografts with human GRPR. The target expression level also has a direct effect on ligand retention. No data have been published on the retention of radioactivity in low and high GRPR-expressing xenografts injected with antagonists. However, it has been shown that the retention of HER2-binding affibody molecules with K_D values of 116.7 ± 0.1 and 157 ± 4 pM in xenografts with high receptor expression (SKOV-3) is longer than the retention of the same high-affinity ligand in low HER2-expressing xenografts (LS174T).[49] Therefore, the long tumor retention of our radiolabeled bombesin analog may also be the result of high GRPR expression on PC-3 cells or a combination of both of these factors.

The high potential of our radiolabeled conjugates for the visualization of GRPR-positive tumors was confirmed by gamma-camera and microPET/CT images. Our biodistribution studies suggest that the optimal time point for image acquisition falls between 2 and 3 h p.i., at which time high tumor-to-receptor-positive organ and tumor-to-kidney ratios were obtained. The best image contrast, which is the most important parameter for informative clinical images, was obtained for the ^{68}Ga-labeled analog at 2 h p.i.

In comparison with the biodistribution data reported for ^{111}In-RM1[24] and ^{111}In/ ^{68}Ga-RM2[25] (1 h p.i.), the ^{111}In/^{68}Ga-NOTA-P2-RM26 variants had (i) the same blood clearance rates, (ii) a slightly higher liver uptake than that of ^{111}In/ ^{68}Ga-RM2[25], and (iii) an up to 5-fold lower pancreas uptake. The uptake of radiolabeled bombesin analogs in the pancreas is known to decrease as the lipophilicity of the conjugate decreases.[45] The lower pancreas uptake of ^{68}Ga-NOTA-P2-RM26 resulted in enhanced contrast in the abdominal area, which has the highest

likelihood for the visualization of distant soft tissue metastases, in comparison with ^{68}Ga-labeled RM2. Liver metastases are not infrequent, but because they appear to be a fairly late event for PC patients, we did not attempt imaging at that late stage.[50] Taken together, the results of this study and the data in the literature suggest that small modifications in the chelator and/or in the linker conjugating the chelator to the peptide can appreciably alter the targeting properties of the peptide.

CONCLUSION

We have developed a peptide-based imaging agent for the visualization of GRPR-expressing tumors using PET and SPECT. This tracer should undergo further clinical consideration to overcome the deficiencies of widely used metabolic PET tracers, such as [^{18}F]-FDG, [^{11}C]-choline, and [^{11}C]-acetate, for PC imaging.

ASSOCIATED CONTENT

Supporting Information

Peptide synthesis; Table S1. Biodistribution of ^{68}Ga-NOTA-P2-RM26 and ^{111}In-NOTA-P2-RM26 (total injected mass of 23 pmol) after injection in male NMRI mice; Table S2. Dose escalation study in BALB/c nu/nu male mice bearing PC-3 xenografts at 2 h p.i. of ^{111}In-NOTA-P2-RM26; Table S3. Biodistribution of ^{68}Ga-NOTA-P2-RM26 and ^{111}In-NOTA-P2-RM26 (total injected mass of 45 pmol) after injection in male BALB/c nu/nu mice bearing PC-3 xenografts; Figure S1. Results of the HPLC and LC-MS analyses of NOTA-P2-RM26; Figure S2. Results of the HPLC analysis of ^{68}Ga-NOTA-P2-RM26; Figure S3. SDS-PAGE analysis of ^{68}Ga-NOTA-P2-RM26 and ^{111}In-NOTA-P2-RM26 after 1 h of incubation with a 500-fold molar excess of EDTA at RT; Figure S4. Real-time kinetics of the peptide/cell surface receptor interactions in intact PC-3 cells for ^{111}In-NOTA-P2-RM26. This material is available free of charge via the Internet at http://pubs.acs.org.

AUTHOR INFORMATION

Corresponding Author

*E-mail: anna.orlova@pet.medchem.uu.se, Fax: +46(0)18 471 5307, Phone: +46(0)73 9922 846.

Notes

The authors declare no competing financial interests.

ACKNOWLEDGMENTS

This research was financially supported by the Swedish Cancer Society (Cancerfonden) and the Swedish Research Council (Vetenskapsrådet).

ABBREVIATIONS

BN, bombesin; DOTA, 1,4,7,10-tetraazacyclododecane-1,4,7,10-tetraacetic acid; GRPR, gastrin-releasing peptide receptor; HPLC, high-performance liquid chromatography; ITLC, instant thin-layer chromatography; R_f ratio of spot migration:mobile phase migration; NOTA, 1,4,7-triazacyclononane-1,4,7-triacetic acid; NOTA-P2-RM26, NOTA-PEG$_2$-[D-Phe^6,Sta^{13},Leu^{14}]bombesin[6−14]; PEG, polyethylene glycol; PC, prostate cancer; PET, positron emission tomography; p.i., post injection; RT, room temperature; SDS-PAGE, sodium dodecyl sulfate-polyacrylamide gel electrophoresis; SPECT, single photon emission computed tomography; %ID/g, percentage of injected dose per gram of tissue

REFERENCES

(1) Ciatto, S., Zappa, M., Bonardi, R., and Gervasi, G. (2000) Prostate cancer screening: the problem of overdiagnosis and lessons to be learned from breast cancer screening. *Eur J Cancer. 36*, 1347−50.

(2) de Visser, M., van Weerden, W. M., de Ridder, C. M., Reneman, S., Melis, M., Krenning, E. P., and de Jong, M. (2007) Androgen-dependent expression of the gastrin-releasing peptide receptor in human prostate tumor xenografts. *J. Nucl. Med. 48*, 88−93.

(3) Perlmutter, M. A., and Lepor, H. (2007) Androgen deprivation therapy in the treatment of advanced prostate cancer. *Rev Urol. 9*, S3−S8.

(4) Even-Sapir, E. (2005) Imaging of malignant bone involvement by morphologic, scintigraphic, and hybrid modalities. *J. Nucl. Med. 46*, 1356−67.

(5) Ananias, H. J., van den Heuvel, M. C., Helfrich, W., and de Jong, I. J. (2009) Expression of the gastrin-releasing peptide receptor, the prostate stem cell antigen and the prostate-specific membrane antigen in lymph node and bone metastases of prostate cancer. *Prostate 69*, 1101−8.

(6) de Visser, M., van Weerden, W. M., de Ridder, C. M., Reneman, S., Melis, M., Krenning, E. P., and de Jong, M. (2007) Androgen-dependent expression of the gastrin-releasing peptide receptor in human prostate tumor xenografts. *J. Nucl. Med. 48*, 88−93.

(7) Beer, M., Montani, M., Gerhardt, J., Wild, P. J., Hany, T. F., Hermanns, T., Müntener, M., and Kristiansen, G. (2012) Profiling gastrin-releasing peptide receptor in prostate tissues: clinical implications and molecular correlates. *Prostate 72*, 318−25.

(8) Kelloff, G. J., Choyke, P., and Coffey, D. S. (2009) Challenges in clinical prostate cancer: role of imaging. *AJR Am. J. Roentgenol. 192*, 1455−70.

(9) Jensen, R. T., Battey, J. F., Spindel, E. R., and Benya, R. V. (2008) International union of pharmacology. LXVIII. Mammalian bombesin receptors: nomenclature, distribution, pharmacology, signaling and functions in normal and disease states. *Pharmacol. Rev. 60*, 1−42.

(10) Minamino, N., Kangawa, K., and Matsuo, H. (1983) Neuromedin B: a novel bombesin-like peptide identified in porcine spinal cord. *Biochem. Biophys. Res. Commun. 114*, 541−8.

(11) McDonald, T. J., Nilsson, G., Vagne, M., Ghatei, M., Bloom, S. R., and Mutt, V. (1978) A gastrin releasing peptide from the porcine nonantral gastric tissue. *Gut 19*, 767−74.

(12) Nock, B. A., Nikolopoulou, A., Galanis, A., Cordopatis, P., Waser, B., Reubi, J. C., and Maina, T. (2005) Potent bombesin-like peptides for GRP-receptor targeting of tumors with 99mTc: a preclinical study. *J. Med. Chem. 48*, 100−10.

(13) Zhang, X., Cai, W., Cao, F., Schreibmann, E., Wu, Y., Wu, J. C., Xing, L., and Chen, X. (2006) 18F-labeled bombesin analogs for targeting GRP receptor-expressing prostate cancer. *J. Nucl. Med. 47*, 492−501.

(14) Dimitrakopoulou-Strauss, A., Hohenberger, P., Haberkorn, U., Mäcke, H. R., Eisenhut, M., and Strauss, L. G. (2007) 68Ga-labeled bombesin studies in patients with gastrointestinal stromal tumors: comparison with 18F-FDG. *J. Nucl. Med. 48*, 1245−50.

(15) Van de Wiele, C., Dumont, F., Vanden Broecke, R., Oosterlinck, W., Cocquyt, V., Serreyn, R., Peers, S., Thornback, J., Slegers, G., and Dierckx, R. A. (2000) Technetium-99m RP527, a GRP analogue for visualisation of GRP receptor-expressing malignancies: a feasibility study. *Eur. J. Nucl. Med. 27*, 1694−9.

(16) Bodei, L., Ferrari, M., Nunn, A., Llull, J., Cremonesi, M., Martano, L., Laurora, G., Scardino, E., Tiberini, S., Bufi, G., Eato, de Cobelli, O., and Paganelli, G. (2007) 177Lu-AMBA bombesin analogue in hormone refractory prostate cancer patients: a phase I escalation study with single-cycle administrations [abstract]. *Eur. J. Nucl. Med. Mol. Imaging 34* (suppl 2), S221.

(17) Van de Wiele, C., Dumont, F., Dierckx, R. A., Peers, S. H., Thornback, J. R., Slegers, G., and Thierens, H. (2001) Biodistribution and dosimetry of ^{99m}Tc-RP527, a gastrin-releasing peptide (GRP) agonist for the visualization of GRP receptor−expressing malignancies. *J. Nucl. Med. 42*, 1722−7.

(18) Abiraj, K., Mansi, R., Tamma, M. L., Fani, M., Forrer, F., Nicolas, G., Cescato, R., Reubi, J. C., and Maecke, H. R. (2011) Bombesin antagonist-based radioligands for translational nuclear imaging of gastrin-releasing peptide receptor-positive tumors. *J. Nucl. Med. 52*, 1970−8.
(19) Nock, B., Nikolopoulou, A., Chiotellis, E., Loudos, G., Maintas, D., Reubi, J. C., and Maina, T. (2003) [99mTc]Demobesin 1, a novel potent bombesin analogue for GRP receptor-targeted tumour imaging. *Eur. J. Nucl. Med. 30*, 247−58.
(20) Llinares, M., Devin, C., Chaloin, O., Azay, J., Noel-Artis, A. M., Bernad, N., Fehrentz, J. A., and Martinez, J. (1999) Syntheses and biological activities of potent bombesin receptor antagonists. *J. Pept. Res. 53*, 275−83.
(21) de Castiglione, R., and Gozzini, L. (1996) Bombesin receptor antagonists. *Crit. Rev. Oncol. Hematol. 24*, 117−51.
(22) Ginj, M., Zhang, H., Waser, B., Cescato, R., Wild, D., Wang, X., Erchegyi, J., Rivier, J., Mäcke, H. R., and Reubi, J. C. (2006) Radiolabeled somatostatin receptor antagonists are preferable to agonists for in vivo peptide receptor targeting of tumors. *Proc. Natl. Acad. Sci. U. S. A. 103*, 16436−41.
(23) Cescato, R., Maina, T., Nock, B., Nikolopoulou, A., Charalambidis, D., Piccand, V., and Reubi, J. C. (2008) Bombesin Receptor Antagonists May Be Preferable to Agonists for Tumor Targeting. *J. Nucl. Med. 49*, 318−26.
(24) Mansi, R., Wang, X., Forrer, F., Kneifel, S., Tamma, M. L., Waser, B., Cescato, R., Reubi, J. C., and Maecke, H. R. (2009) Evaluation of a 1,4,7,10-tetraazacyclododecane-1,4,7,10-tetraacetic acid-conjugated bombesin-based radioantagonist for the labeling with single-photon emission computed tomography, positron emission tomography, and therapeutic radionuclides. *Clin. Cancer Res. 15*, 5240−9.
(25) Mansi, R., Wang, X., Forrer, F., Waser, B., Cescato, R., Graham, K., Borkowski, S., Reubi, J. C., and Maecke, H. R. (2011) Development of a potent DOTA-conjugated bombesin antagonist for targeting GRPr-positive tumours. *Eur. J. Nucl. Med. Mol. Imaging 38*, 97−107.
(26) Velikyan, I., Maecke, H., and Langstrom, B. (2008) Convenient preparation of ^{68}Ga-based PET-radiopharmaceuticals at room temperature. *Bioconjugate Chem. 19*, 569−73.
(27) Atherton, E., and Sheppard, R. (1989) Fluorenylmethoxycarbonyl-polyamide solid phase peptide synthesis. *General principles and development*, Oxford Information Press, Oxford.
(28) Altai, M., Varasteh, Z., Andersson, K., Eek, A., Boerman, O., and Orlova, A. (2013) In vivo and in vitro studies on renal uptake of radiolabeled affibody molecules for imaging of HER2 expression in tumors. *Cancer Biother. Radiopharm. 28*, 187−95.
(29) Björke, H., and Andersson, K. (2006) Automated, high-resolution cellular retention and uptake studies in vitro. *Appl. Radiat. Isot. 64*, 901−5.
(30) Björke, H., and Andersson, K. (2006) Measuring the affinity of a radioligand with its receptor using a rotating cell dish with in situ reference area. *Appl. Radiat. Isot. 64*, 32−7.
(31) Lawrentschuk, N., Davis, I. D., Bolton, D. M., and Scott, A. M. (2006) Positron emission tomography and molecular imaging of the prostate: an update. *BJU Int. 97*, 923−31.
(32) Mena, E., Turkbey, B., Mani, H., Adler, S., Valera, V. A., Bernardo, M., Shah, V., Pohida, T., McKinney, Y., Kwarteng, G., Daar, D., Lindenberg, M. L., Eclarinal, P., Wade, R., Linehan, W. M., Merino, M. J., Pinto, P. A., Choyke, P. L., and Kurdziel, K. A. (2012) ^{11}C-Acetate PET/CT in localized prostate cancer: a study with MRI and histopathologic correlation. *J. Nucl. Med. 53*, 538−45.
(33) Beheshti, M., Imamovic, L., Broinger, G., Vali, R., Waldenberger, P., Stoiber, F., Nader, M., Gruy, B., Janetschek, G., and Langsteger, W. (2010) ^{18}F choline PET/CT in the preoperative staging of prostate cancer in patients with intermediate or high risk of extracapsular disease: a prospective study of 130 patients. *Radiology 254*, 925−33.
(34) Takahashi, N., Inoue, T., Lee, J., Yamaguchi, T., and Shizukuishi, K. (2007) The roles of PET and PET/CT in the diagnosis and management of prostate cancer. *Oncology 72*, 226−33.
(35) de Visser, M., van Weerden, W. M., de Ridder, C. M., Reneman, S., Melis, M., Krenning, E.P ., and de Jong, M. (2007) Androgen-dependent expression of the gastrin-releasing peptide receptor in human prostate tumor xenografts. *J. Nucl. Med. 48*, 88−93.
(36) Dijkgraaf, I., Franssen, G. M., McBride, W. J., D'Souza, C. A., Laverman, P., Smith, C. J., Goldenberg, D. M., Oyen, W. J., and Boerman, O. C. (2012) PET of tumors expressing gastrin-releasing peptide receptor with an 18F-labeled bombesin analog. NOTA. *J. Nucl. Med. 53*, 947−52.
(37) Prasanphanich, A. F., Nanda, P. K., Rold, T. L., Ma, L., Lewis, M. R., Garrison, J. C., Hoffman, T. J., Sieckman, G. L., Figueroa, S. D., and Smith, C. J. (2007) [^{64}Cu-NOTA-8-Aoc-BBN(7−14)NH2] targeting vector for positron-emission tomography imaging of gastrin-releasing peptide receptor-expressing tissues. *Proc. Natl. Acad. Sci. U. S. A. 104*, 12462−7.
(38) McBride, W. J., D'Souza, C. A., Sharkey, R. M., Karacay, H., Rossi, E. A., Chang, C. H., and Goldenberg, D. M. (2010) Improved ^{18}F labeling of peptides with a fluoride aluminum-chelate complex. *Bioconjugate Chem. 21*, 1331−40.
(39) Zhang, H. (2007) Design, Synthesis, and Preclinical Evaluation of Radiolabeled Bombesin Analogues for the Diagnosis and Targeted Radiotherapy of Bombesinreceptor Expressing Tumors, PhD thesis, Basel University, Basel, Switzerland, http://edoc.unibas.ch/586/1/DissB_7877.pdf.
(40) Shetty, D., Choi, S. Y., Jeong, J. M., Hoigebazar, L., Lee, Y. S., Lee, D. S., Chung, J. K., Lee, M. C., and Chung, Y. K. (2010) Formation and characterization of gallium(III) complexes with monoamide derivatives of 1,4,7-triazacyclononane-1,4,7-triacetic acid: a study of the dependency of structure on reaction pH. *Eur. J. Inorg. Chem. 34*, 5432−8.
(41) Schuhmacher, J., Zhang, H., Doll, J., Mäcke, H. R., Matys, R., Hauser, H., Henze, M., Haberkorn, U., and Eisenhut, M. (2005) GRP receptor-targeted PET of a rat pancreas carcinoma xenograft in nude mice with a ^{68}Ga-labeled bombesin(6−14) analog. *J. Nucl. Med. 46*, 691−9.
(42) Schroeder, R. P., De Blois, E., De Ridder, C. M., Van Weerden, W. M., Breeman, W. A., and de Jong, M. (2012) Improving radiopeptide pharmacokinetics by adjusting experimental conditions for bombesin receptor-targeted imaging of prostate cancer. *Q. J. Nucl. Med. Mol. Imaging 56*, 468−75.
(43) Koumarianou, E., Mikołajczak, R., Pawlak, D., Zikos, X., Bouziotis, P., Garnuszek, P., Karczmarczyk, U., Maurin, M., and Archimandritis, S. C. (2009) Comparative study on DOTA-derivatized bombesin analog labeled with 90Y and 177Lu: in vitro and in vivo evaluation. *Nucl. Med. Biol. 36*, 591−603.
(44) Zhang, H., Schuhmacher, J., Waser, B., Wild, D., Eisenhut, M., Reubi, J. C., and Maecke, H. R. (2007) DOTA-PESIN, a DOTA-conjugated bombesin derivative designed for the imaging and targeted radionuclide treatment of bombesin receptor-positive tumours. *Eur. J. Nucl. Med. Mol. Imaging 34*, 1198−208.
(45) Hoffman, T. J., Gali, H., Smith, C. J., Sieckman, G. L., Hayes, D. L., Owen, N. K., and Volkert, W. A. (2003) Novel series of ^{111}In-labeled bombesin analogs as potential radiopharmaceuticals for specific targeting of gastrin-releasing peptide receptors expressed on human prostate cancer cells. *J. Nucl. Med. 44*, 823−31.
(46) Maddalena, M. E., Fox, J., Chen, J., Feng, W., Cagnolini, A., Linder, K. E., Tweedle, M. F., Nunn, A. D., and Lantry, L. E. (2009) 177Lu-AMBA biodistribution, radiotherapeutic efficacy, imaging, and autoradiography in prostate cancer models with low GRP-R expression. *J. Nucl. Med. 50*, 2017−24.
(47) Giladi, E., Nagalla, S. R., and Spindel, E. R. (1993) Molecular cloning and characterization of receptors for the mammalian bombesin-like peptides. *J. Mol. Neurosci. 4*, 41−54.
(48) Maina, T., Nock, B. A., Zhang, H., Nikolopoulou, A., Waser, B., Reubi, J. C., and Maecke, H. R. (2005) Species differences of bombesin analog interactions with GRP-R define the choice of animal models in the development of GRP-R-targeting drugs. *J. Nucl. Med. 46*, 823−30.

(49) Tolmachev, V., Tran, T. A., Rosik, D., Sjöberg, A., Abrahmsén, L., and Orlova, A. (2012) Tumor targeting using affibody molecules: interplay of affinity, target expression level, and binding site composition. *J. Nucl. Med. 53*, 953−60.
(50) Pouessel, D., Gallet, B., Bibeau, F., Avancès, C., Iborra, F., Sénesse, P., and Culine, S. (2007) Liver metastases in prostate carcinoma: clinical characteristics and outcome. *BJU Int. 99*, 807−11.